$b \to s\gamma$ confronts B-violating scalar couplings: R-parity violating supersymmetry or diquarks

Debrupa Chakraverty* and Debajyoti Choudhury†
Mehta Research Institute, Chhatnag Road, Jhusi, Allahabad 211 019, India
(Received 22 August 2000; published 7 March 2001)

We investigate the possible role that baryon number violating Yukawa interactions may take in the inclusive decay $B \to X_s\gamma$. The constraints, derived using the experimental results of the CLEO Collaboration, turn out, in many cases, to be more stringent than the existing bounds.

DOI: 10.1103/PhysRevD.63.075009 PACS number(s): 12.60.Jv, 13.20.He, 13.25.Hw

The standard model (SM) of the strong, weak, and electromagnetic interactions is in very good agreement with almost all present experimental data, even though a few important predictions have not yet been tested. Still, most physicists would readily admit that the SM cannot be the final theory, both on aesthetic grounds as well as on account of certain well-founded technical objections. As a result, numerous attempts have been and are being made in the quest of a more fundamental theory. Experimentally, there have been two main strategies to probe new physics. On the one hand, we attempt to directly produce and observe new particles at high energy colliders. On the other, we look for virtual effects of such particles and/or interactions in various low and intermediate energy processes. The decay $b \to s\gamma$ is an excellent candidate for the latter option [1–14]. Experimentally, the branching ratio for the inclusive decay $B \to X_s\gamma$ has been measured by CLEO [15] and ALEPH [16] to be

$$BR(B \to X_s\gamma) = \begin{cases} (3.15 \pm 0.93) \times 10^{-4} & \text{(CLEO)}, \\ (3.11 \pm 1.52) \times 10^{-4} & \text{(ALEPH)}. \end{cases} \tag{1}$$

The above are in good agreement with each other and with the SM prediction [17] of $BR(B \to X_s\gamma) = (3.29 \pm 0.33) \times 10^{-4}$. While a small window for the contribution of new physics does remain, this agreement can obviously be used to constrain deviations from the SM.

In this paper, we investigate the influence that a scalar diquark may have on the above decay.[1] Diquarks abound in many grand unified theories (with or without supersymmetry) and even in composite models [18]. While vector diquarks are constrained to be superheavy[2] (with masses of the scale of breaking of the additional gauge symmetry), no such restrictions apply to the masses of scalar diquarks. Consequently, such particles can be as light as the electroweak scale. For example, a diquark like behavior can be found even in a low energy theory such as the minimal supersymmetric standard model (MSSM), albeit in the version with broken R-parity.

A generic diquark is a scalar or vector particle that couples to a quark current with a net baryon number $B = \pm 2/3$. Clearly, it may transform as either a $SU(3)_c$ triplet or a sextet. Concentrating on the scalars (for reasons mentioned above), the generic Yukawa term in the Lagrangian can be expressed as

$$\mathcal{L}_Y^{(A)} = h_{ij}^{(A)} \overline{q_i^c} P_{L,R} q_j \Phi_A + \text{H.c.}, \tag{2}$$

where i,j denote quark flavors, A denotes the diquark type and $P_{L,R}$ reflect the quark chirality. Standard model gauge invariance demands that a scalar diquark transform either as a triplet or as a singlet under $SU(2)_L$ and that it have a $U(1)$ hypercharge $|Y| = \frac{2}{3}, \frac{4}{3}, \frac{8}{3}$. The full list of quantum numbers is presented in Table I. It is clear that the couplings $h_{ij}^{(1)}$, $h_{ij}^{(4)}$, $h_{ij}^{(5)}$, and $h_{ij}^{(7)}$ must be symmetric under the exchange of i and j while $h_{ij}^{(2)}$, $h_{ij}^{(3)}$, $h_{ij}^{(6)}$, and $h_{ij}^{(8)}$ must be antisymmetric under the same exchange. For the other two sets of couplings, viz. $\tilde{h}_{ij}^{(3)}$ and $\tilde{h}_{ij}^{(4)}$, there is no particular symmetry property. Note that the quantum numbers of $\Phi_{2,4,6}$ allow them to couple to a leptoquark (i.e., a quark-lepton) current as well. This implies that these particular diquarks could also mediate lepton-number (L) violating processes. Clearly, in order to coexist with non-negligible B violating diquark couplings, such leptoquark couplings need to be suppressed severely so as to prevent rapid proton decay.

We make a brief interlude here to discuss the MSSM [19]. Whereas B and L are (accidentally) preserved in the SM (at least in the perturbative context), it is not so within the MSSM. Supersymmetry and gauge invariance, together with the field content, allow terms in the superpotential that violate either B or L [20]. Catastrophic rates for proton decay can be avoided though by imposing a global Z_2 symmetry [21] under which the quark and lepton superfields change by a sign, while the Higgs superfields remain invariant. Representible as $R \equiv (-1)^{3B-L+2S}$, where S is the spin of a field, this ''R-parity'' is positive for the SM fields and negative for all the supersymmetric partners. However, while this symmetry is useful in preventing phenomenologically unacceptable terms, it has no theoretical foundation and is entirely *ad hoc* in nature. Hence, it is of interest to examine the conse-

*Email address: rupa@mri.ernet.in
†Email address: debchou@mri.ernet.in

[1]A brief discussion on the sensitivity of the branching ratio $B \to X_s\gamma$ to scalar diquark-top contribution has been presented in Ref. [17].

[2]We do not consider the case of nongauged vector diquarks as such theories are nonrenormalizable.

TABLE I. Gauge quantum numbers and Yukawa couplings of scalar diquarks ($Q_{em}=T_3+Y/2$).

Diquark type	Coupling	$SU(3)_c\times SU(2)_L\times U(1)_Y$
Φ_1	$h_{ij}^{(1)}(\overline{Q}_{Li})^c Q_{Lj}\Phi_1$	$(\overline{6},\ 3,\ -\frac{2}{3})$
Φ_2	$h_{ij}^{(2)}(\overline{Q}_{Li})^c Q_{Lj}\Phi_2$	$(3,\ 3,\ -\frac{2}{3})$
Φ_3	$[h_{ij}^{(3)}(\overline{Q}_{Li})^c Q_{Lj}+\tilde{h}_{ij}^{(3)}(\overline{u}_{Ri})^c d_{Rj}]\Phi_3$	$(\overline{6},\ 1,\ -\frac{2}{3})$
Φ_4	$[h_{ij}^{(4)}(\overline{Q}_{Li})^c Q_{Lj}+\tilde{h}_{ij}^{(4)}(\overline{u}_{Ri})^c d_{Rj}]\Phi_4$	$(3,\ 1,\ -\frac{2}{3})$
Φ_5	$h_{ij}^{(5)}(\overline{u}_{Ri})^c u_{Rj}\Phi_5$	$(\overline{6},\ 1,\ -\frac{8}{3})$
Φ_6	$h_{ij}^{(6)}(\overline{u}_{Ri})^c u_{Rj}\Phi_6$	$(3,\ 1,\ -\frac{8}{3})$
Φ_7	$h_{ij}^{(7)}(\overline{d}_{Ri})^c d_{Rj}\Phi_7$	$(\overline{6},\ 1,\ \frac{4}{3})$
Φ_8	$h_{ij}^{(8)}(\overline{d}_{Ri})^c d_{Rj}\Phi_8$	$(3,\ 1,\ \frac{4}{3})$

quences of violating this symmetry, not in the least because it plays a crucial role in the search for supersymmetry. In our study, we shall restrict ourselves to the case where only the B-violating terms are nonzero. Such scenarios can be motivated within a class of supersymmetric grand unified theories (GUT) as well [22]. The corresponding terms in the superpotential can be parametrized as

$$W_{\not{R}}=\lambda''_{ijk}\overline{U}^i_R\overline{D}^j_R\overline{D}^k_R, \tag{3}$$

where $\overline{U}^i_R$ and $\overline{D}^i_R$ denote the right-handed up-quark and down-quark superfields, respectively. The couplings λ''_{ijk} are antisymmetric under the exchange of the last two indices. The corresponding Lagrangian can then be written in terms of the component fields as

$$\mathcal{L}_{\not{R}}=\lambda''_{ijk}(u_i^c d_j^c \tilde{d}_k^* + u_i^c\tilde{d}_j^* d_k^c+\tilde{u}_i^* d_j^c d_k^c)+\text{H.c.} \tag{4}$$

Thus, a single term in the superpotential corresponds to *three different* diquark interactions, namely, two of type $\tilde{h}_{ij}^{(4)}$ and one of type $h_{ij}^{(8)}$.

The best direct bound on diquark type couplings comes from the analysis of dijet events by the Collider Detector at Fermilab (CDF) Collaboration [23]. Considering the process $q_iq_j\to\Phi_A\to q_iq_j$, an exclusion curve in the $(m_{\Phi_A},h_{ij}^{(A)})$ plane can be obtained from this data. Two points need to be noted though. At a $p\overline{p}$ collider like the Tevatron, the uu and dd fluxes are small and hence the bounds obtained are relatively weak. This is even more so for quarks of the second or third generation (which are relevant for the couplings that we are interested in). Secondly, such an analysis needs to make assumptions regarding the branching fraction of Φ_A into quark pairs, a point that is of particular importance in the context of R-parity violating supersymmetric models.

TABLE II. 1σ upper bounds on the individual scalar diquark couplings for $m_{\Phi_i}=100$ GeV from Refs. [24] and [29].

Couplings	Limits	Couplings	Limits
$h_{33}^{(1)}$	0.35	$\tilde{h}_{33}^{(3)}$	1.12
$h_{23}^{(1)}$	0.89	$\tilde{h}_{32}^{(3)}$	1.11
$h_{23}^{(3)}$	0.54	λ''_{312}	0.50
$h_{33}^{(4)}$	0.60	λ''_{313}	0.50
$h_{23}^{(4)}$	0.66	λ''_{323}	0.50

There also exist some constraints derived from low energy processes. Third generation couplings, for example, can be constrained from the precision electroweak data at the CERN $e^{\dagger}e^-$ collider LEP [24] or, to an extent, by demanding perturbative unitarity to a high scale [25]. Couplings involving the first two generations, on the other hand, are constrained[3] by the nonobservance of neutron-antineutron oscillations or from an analysis of rare nucleon and meson decays [26,27]. While many of these individual bounds are weak, certain of their *products* are much more severely constrained by the data on neutral meson mixing and CP violation in the K sector [28]. We have displayed the best upper bound on the relevant individual Yukawa couplings in Table II. It is our aim, in this article, to derive analogous, but, stronger bounds.

Within the SM, the quark level transition $b\to s\gamma$ is mediated, at the lowest order, by electromagnetic penguin diagrams shown in Figs. 1(a)–1(d). While only the top-quark diagrams have been shown, for consistency's sake, other charge 2/3 quarks should also be included. However, these contributions are negligible on two counts: (i) the small mixing angles and (ii) the corresponding loop integrals being suppressed to a great extent due to the smallness of the light quark masses. The matrix element for this process is then governed by the dipole operator:

$$-\frac{4G_F}{\sqrt{2}}V_{ts}^*V_{tb}\left(\frac{e}{32\pi^2}\right)C_7^{\text{SM}}(m_W)\overline{s}\sigma_{\mu\nu}F^{\mu\nu}[m_b(1+\gamma_5)]b. \tag{5}$$

The QCD corrections to this process are calculated via an operator product expansion based on the effective Hamiltonian

$$H_{\text{eff}}=-\frac{4G_F}{\sqrt{2}}V_{ts}^*V_{tb}\sum_{i=1}^{8}C_i(\mu)O_i(\mu), \tag{6}$$

[3]Although many of these analyses have been done for the case of R-parity violating models, clearly similar bounds would also apply to nonsupersymmetric diquark couplings as well.

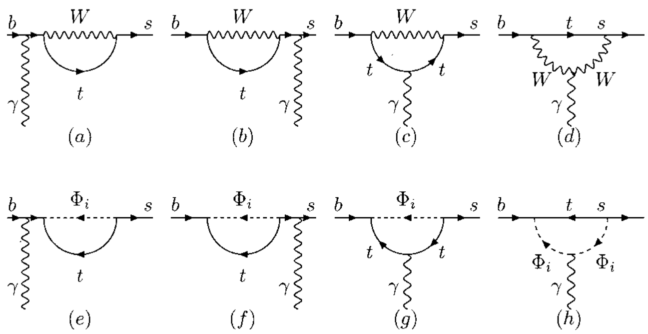

FIG. 1. Feynman diagrams that determine the one loop $b \to s\gamma$ decay amplitude.

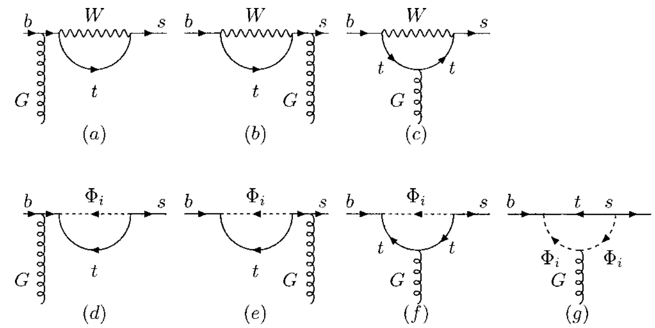

FIG. 2. Feynman diagrams that determine the one loop $b \to sG$ decay amplitude.

which is then evolved from the electroweak scale down to $\mu = \mu_b$ through renormalization group (RG) equations. A large correction owes itself to the chromomagnetic operator $b \to sG$ (G being a gluon)

$$-\frac{4G_F}{\sqrt{2}} V_{ts}^* V_{tb} \left(\frac{g_s}{32\pi^2} \right) C_8^{\rm SM}(m_W) \overline{s}_\alpha \sigma_{\mu\nu} G^{\mu\nu}_{\alpha\beta} [m_b(1+\gamma_5)] b_\beta , \tag{7}$$

which arises from the diagrams of Figs. 2(a)–2(c). The Wilson coefficients $C_7^{\rm SM}(m_W)$ and $C_8^{\rm SM}(m_W)$ can be evaluated perturbatively [30–32] at the m_W scale where the matching conditions are imposed. The explicit expressions are

$$C_7^{\rm SM}(m_W) = x \left[\frac{7-5x-8x^2}{24(x-1)^3} + \frac{x(3x-2)}{4(x-1)^4} \ln x \right],$$

$$C_8^{\rm SM}(m_W) = x \left[\frac{2+5x-x^2}{8(x-1)^3} - \frac{3x}{4(x-1)^4} \ln x \right], \tag{8}$$

where $x = m_t^2 / m_W^2$.

The leading order result for the relevant Wilson coefficient at μ_b, the B-meson scale, is given by

$$C_7(\mu_b) = \eta^{16/23} \left[C_7^{\rm SM}(m_W) - \frac{8}{3} C_8^{\rm SM}(m_W)(1-\eta^{-2/23}) + \frac{232}{513}(1-\eta^{-19/23}) \right] \tag{9}$$

with $\eta \equiv \alpha_s(m_W)/\alpha_s(\mu_b)$, calculated using the leading μ dependence of α_s, and the present world average value of the strong coupling constant viz. $\alpha_s(m_Z) = 0.118 \pm 0.005$. To this order, then,

$$\Gamma(b \to s\gamma) = \frac{\alpha G_F^2 m_b^5}{32\pi^4} \left| V_{tb} V_{ts}^* C_7^{\rm SM}(\mu_b) \right|^2 , \tag{10}$$

where α is the fine structure constant. As the above decay rate suffers from large uncertainties due to m_b and the Cabibbo-Kobayashi-Masakawa (CKM) matrix elements, it is prudent to normalize it against the measured semileptonic decay rate of the b quark

$$\Gamma(b \to c e \overline{\nu}_e) = \frac{G_F^2 m_b^5}{192\pi^3} \kappa(z) g(z) |V_{cb}|^2 , \tag{11}$$

where $z = m_c^2 / m_b^2$ and

$$g(z) \equiv 1 - 8z + 8z^2 - z^4 - 12z^2 \ln z$$

is the phase space factor. The analytic expression for $\kappa(z)$, the one loop QCD correction to the semileptonic decay, can be found in Ref. [33]. The explicit dependence on m_b^5 is thus removed, while the ratio of the CKM elements in the scaled decay rate, viz.,

$$\left| \frac{V_{ts}^* V_{tb}}{V_{cb}} \right| = 0.976 \pm 0.010 \tag{12}$$

is much better determined than the individual elements.

An updated, next to leading order (NLO), analysis [33] of the $B \to X_s \gamma$ branching ratio with QED corrections has been presented in Ref. [17]. Incorporating both the NLO QCD and the resummed QED corrections, the Wilson coefficient $C_7^{\rm eff}(\mu_b)$ in SM can be expanded as

$$C_7^{\rm eff}(\mu_b) = C_7(\mu_b) + \frac{\alpha_s(\mu_b)}{4\pi} C_7^{(1)}(\mu_b) + \frac{\alpha}{\alpha_s(\mu_b)} C_7^{(em)}(\mu_b). \tag{13}$$

For brevity's sake, we do not give here the expressions for $C_7^{(1)}(\mu_b)$ and $C_7^{(em)}(\mu_b)$ as these can be found in Ref. [33] and Ref. [17], respectively. The inclusion of the NLO and QED corrections in the $b \to s\gamma$ decay rate significantly reduces the large uncertainty present in the LO calculation. From the quark level $b \to s\gamma$ decay rate, it is possible to infer the B meson inclusive branching ratio $BR(B \to X_s \gamma)$ by including the nonperturbative $1/m_b$ and $1/m_c$ corrections. These bound state corrections have also been taken into account in Ref. [17].

Having delineated the formalism, it now remains to calculate the additional contributions due to the possible presence of nonzero diquark couplings. At the one-loop level, the only new contributions to $b \to s\gamma$ and $b \to sG$ arise from the diagrams of Figs. 1(e)–1(h) and Figs. 2(d)–2(g), respectively.[4] In the generic case, apart from modifications in the coefficients of $O_{7,8}$, two additional operators arise. Denoted as

$$\tilde{O}_7 = \frac{e}{32\pi^2}\bar{s}\sigma_{\mu\nu}F^{\mu\nu}[m_b(1-\gamma_5)]b,$$

$$\tilde{O}_8 = \frac{g_s}{32\pi^2}\bar{s}_\alpha\sigma_{\mu\nu}G^{\mu\nu}_{\alpha\beta}[m_b(1-\gamma_5)]b_\beta, \tag{14}$$

they differ from their SM counterparts only in their chirality structure.[5]

To keep the analysis simple, we shall assume that only one diquark multiplet is light and that all the fields within a multiplet are degenerate.[6] With this simplifying assumption, the new contributions, at the electroweak scale, are given by

$$C_7^D(m_W) = \frac{N_c}{\mathcal{A}}\left[\{Q_\Phi F_1(y) + Q_t F_3(y)\} l_b l_s^* + \frac{m_t}{m_b}\{Q_t F_4(y) - Q_\Phi F_2(y)\} r_b l_s^*\right],$$

$$\tilde{C}_7^D(m_W) = \frac{N_c}{\mathcal{A}}\left[\{Q_\Phi F_1(y) + Q_t F_3(y)\} r_b r_s^* + \frac{m_t}{m_b}\{Q_t F_4(y) - Q_\Phi F_2(y)\} l_b r_s^*\right],$$

$$C_8^D(m_W) = \mathcal{A}^{-1}\left[\{C_\Phi F_1(y) + C_t F_3(y)\} l_b l_s^* + \frac{m_t}{m_b}\{C_t F_4(y) - C_\Phi F_2(y)\} r_b l_s^*\right],$$

$$\tilde{C}_8^D(m_W) = \mathcal{A}^{-1}\left[\{C_\Phi F_1(y) + C_t F_3(y)\} r_b r_s^* + \frac{m_t}{m_b}\{C_t F_4(y) - C_\Phi F_2(y)\} l_b r_s^*\right],$$

$$\mathcal{A} \equiv -4\sqrt{2}G_F V_{ts}^* V_{tb} m_\Phi^2, \tag{15}$$

where

$$F_1(y) = \frac{1}{12(y-1)^4}[6y^2\ln y - 2y^3 - 3y^2 + 6y - 1],$$

$$F_2(y) = \frac{1}{2(y-1)^3}[1 - y^2 + 2y\ln y],$$

$$F_3(y) = \frac{1}{12(y-1)^4}[2 + 3y - 6y^2 + y^3 + 6y\ln y],$$

$$F_4(y) = \frac{1}{2(1-y)^3}[3 - 4y + y^2 + 2\ln y], \tag{16}$$

with $y = m_t^2/m_\Phi^2$. The color factor N_c is -1 and 2 for triplet and $\bar{6}$ scalar, respectively. Q_t and Q_Φ are the charges of top quark and the diquark, respectively. The color factors C_t and C_Φ—for the diagrams of Figs. 2(f) and 2(g)—are given in Table III.

TABLE III. Values of the coefficients C_Φ, C_t, and chiral Yukawa couplings for different types of scalar diquarks.

Diquark type	C_Φ	C_t	l_b	l_s	r_b	r_s
Φ_1	$-5/2$	1/2	$h_{33}^{(1)}/\sqrt{2}$	$h_{32}^{(1)}/\sqrt{2}$	0	0
Φ_2	1/2	1/2	0	$h_{32}^{(2)}/\sqrt{2}$	0	0
Φ_3	$-5/2$	1/2	0	$h_{32}^{(3)}$	$\tilde{h}_{33}^{(3)}$	$\tilde{h}_{32}^{(3)}$
Φ_4	1/2	1/2	$h_{33}^{(4)}$	$h_{32}^{(4)}$	$\tilde{h}_{33}^{(4)}$	$\tilde{h}_{32}^{(4)}$

Note that, once again, we consider only such contributions, as involve the top quark. As is easy to ascertain from Eq. (15), for other quarks in the loop, the corresponding integrals are too small to be of any consequence. Thus, any coupling to the diquarks $\Phi_{7,8}$, for example, would not be constrained to an appreciable degree by radiative b decays. Furthermore, the diquark Φ_2 does not contribute to $b \to s\gamma$ due to the antisymmetric property of $h_{ij}^{(2)}$. In Table III, we also display the relevant chiral Yukawa couplings (to the b and s quarks) for different choices of the diquark. For our numerical results, we will assume these couplings to be real.[7]

In estimating the effects of scalar diquark couplings, it is useful to consider the ratios [17] $\xi_{7,8}$ with

$$\xi_7 \equiv 1 + \frac{C_7^D(m_W)}{C_7^{\rm SM}(m_W)}, \tag{17}$$

and similarly for ξ_8. For the new operators $\tilde{O}_7$ and $\tilde{O}_8$, we define

$$\tilde{\xi}_7 = \frac{\tilde{C}_7^D(m_W)}{C_7^{\rm SM}(m_W)} \tag{18}$$

and $\tilde{\xi}_8$ in an analogous fashion. With these definitions, the $B \to X_s\gamma$ branching ratio can be written as

$$BR(B\to X_s\gamma) = B_{22}(\delta) + (\xi_7^2 + \tilde{\xi}_7^2)B_{77}(\delta) + (\xi_8^2 + \tilde{\xi}_8^2)B_{88}(\delta) + \xi_7 B_{27}(\delta) + \xi_8 B_{28}(\delta) + (\xi_7\xi_8 + \tilde{\xi}_7\tilde{\xi}_8)B_{78}(\delta). \tag{19}$$

[4]Clearly, to this order, none of $\Phi_{5,6}$ can mediate either of these processes and hence we shall not consider such fields any further.

[5]In all of these four operators, contributions proportional to the strange quark mass have been neglected.

[6]Large splittings within a multiplet is disfavored by the electroweak precision data.

[7]The extension to complex couplings is straightforward. The imaginary parts, however, can be better constrained from an analysis of the CP violating decay modes.

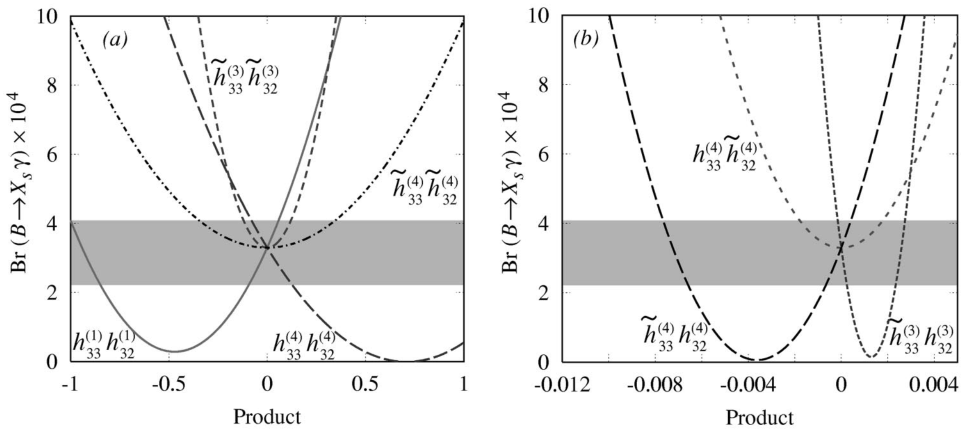

FIG. 3. The partial width for $B\to X_s\gamma$ as a function of the product of the diquark and/or R parity violating couplings for a fixed diquark mass of 100 GeV. The shaded region represents the 1σ limits of the experimentally observed value.

In a parton level analysis, the photon would be monochromatic, with $E_\gamma = E_\gamma^{\max} = m_b/2$. However, once the gluon Bremsstrahlung contribution is included, the photon spectrum becomes nontrivial and, for experimental purposes, one needs to make an explicit demand on the photon energy, namely

$$E_\gamma > (1-\delta)E_\gamma^{\max}, \tag{20}$$

where δ is the fraction of the spectrum above the cut. The values for $B_{ij}(\delta)$ are listed in Ref. [17] for different choices of the renormalization scale μ_b and the photon energy cutoff parameter δ. As is well known, some ambiguities exist in the choice of μ_b which should, typically, lie in the region $m_b/2$ to $2m_b$. For our analysis, we used the values of $B_{ij}(\delta)$ for $\mu_b = m_b$ and $\delta = 0.9$ from Ref. [17]. We have checked that the $B_{ij}(\delta)$'s for other values of δ (listed in Ref. [17]) do not alter the bound significantly.

Since the new physics becomes operative only above the electroweak scale, the additional contributions to the operators O_7 and O_8 will serve only to change the Wilson coefficients at m_W.

Of course, the additional operators $\tilde{O}_7$ and $\tilde{O}_8$ would influence the RG equations for C_7 and C_8 as well. However, since we are primarily interested in small $C^D_{7,8}(m_W)$, it is safe to neglect any term in the RG equations involving these particular coefficients.

In the absence of an L-violating coupling, these diquarks clearly do not influence the semileptonic decay modes of the B meson. Thus, we may continue to normalize the radiative b-decay against $b\to ce\overline{\nu_e}$ in order to avoid the severe dependence on m_b. In Fig. 3, we plot the branching ratio $BR(B\to X_s\gamma)$ in presence of a diquark (multiplet) of mass 100 GeV. We continue to work under the assumption that only one pair of couplings is nonzero. That the curves should be parabolic in the product of the two couplings in question is obvious. To appreciate the fact that many of these curves have their minimum coincide with the SM value, one needs to consider the chirality structure of the corresponding diquark couplings (see Table III). For example, combinations involving either of $\tilde{h}^{(3)}_{32}$ or $\tilde{h}^{(4)}_{32}$ scalar couplings to the strange quark involve only the s_R. From Eqs. (15), it is then easy to see that the Wilson coefficients $C_{7,8}$ remain unaltered from

TABLE IV. Limits on the scalar diquark couplings for $m_{\Phi_i} = 100$ GeV.

Products of couplings	Bounds from $B\to X_s\gamma$ 1σ	2σ
$h^{(1)}_{33}h^{(1)}_{32}$	$[-1.0,-0.85]$ $[-9.3\times10^{-2},5.8\times10^{-2}]$	$[-1.1,-0.74]$ $[-0.2,0.12]$
$\tilde{h}^{(3)}_{33}h^{(3)}_{32}$	$[-1.5\times10^{-4},2.4\times10^{-4}]$ $[2.3\times10^{-3},2.7\times10^{-3}]$	$[-3.1\times10^{-4},5.1\times10^{-4}]$ $[2.1\times10^{-3},2.9\times10^{-3}]$
$\tilde{h}^{(3)}_{33}\tilde{h}^{(3)}_{32}$	$[-0.12,0.12]$	$[-0.18,0.18]$
$h^{(4)}_{33}h^{(4)}_{32}$	$[-8.0\times10^{-2},0.13]$ $[1.3,1.5]$	$[-0.16,0.26]$ $[1.1,1.6]$
$h^{(4)}_{33}\tilde{h}^{(4)}_{32}$	$[-1.8\times10^{-3},1.8\times10^{-3}]$	$[-2.6\times10^{-3},2.6\times10^{-3}]$
$\tilde{h}^{(4)}_{33}h^{(4)}_{32}$	$[-7.7\times10^{-3},-6.6\times10^{-3}]$ $[-6.6\times10^{-4},4.2\times10^{-4}]$	$[-8.1\times10^{-3},-5.8\times10^{-3}]$ $[-1.4\times10^{-3},8.6\times10^{-4}]$
$\tilde{h}^{(4)}_{33}\tilde{h}^{(4)}_{32}$	$[-0.35,0.35]$	$[-0.51,0.51]$

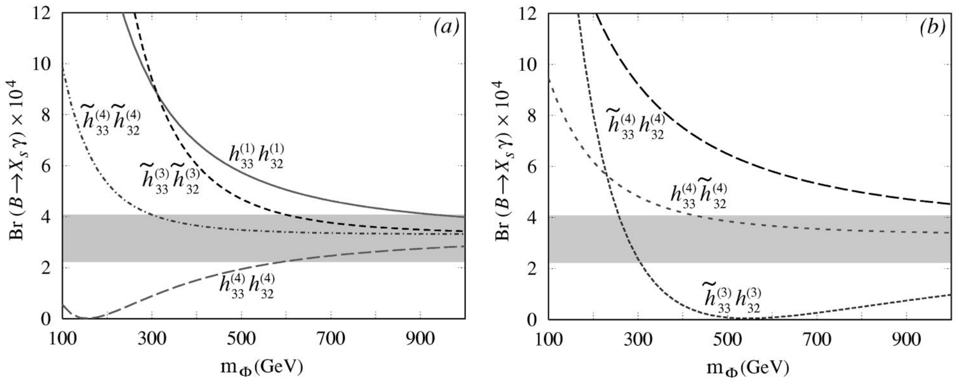

FIG. 4. The partial width for $B \to X_s\gamma$ as a function of diquark mass. (a) For each curve, the associated product of diquark and/or R parity violating couplings is held to be 1, while all other couplings are set to be vanishingly small. The shaded region represents the 1σ limits of the observed value. (b) As in (a), but the nonzero products of diquark and/or R parity violating couplings are held to be 0.005.

their SM value. Consequently, the new contribution adds *incoherently* with the SM amplitude. For the rest of the combinations, though, the interference term is nonnegligible leading to a shift in the minimum. Hence, unlike those for the first set of combinations (ones involving $\tilde{h}_{32}^{(3,4)}$), the branching ratios corresponding to these sets are in agreement with the experimental numbers for *two non-contiguous* ranges of the product.

In each of Eqs. (15), the second term, whenever allowed, is clearly the dominant piece. This enhancement by the factor of m_t/m_b comes into play only when the diquark couplings to the bottom and the strange quarks have pieces with opposite chirality. In other words, for a diquark of the type Φ_3 (or Φ_4), the simultaneous presence of both the allowed types of couplings is severely constrained by the data on $B \to X_s\gamma$.

In Table IV, we capture the essence of Fig. 3 in the form of actual limits that can be set on such products of couplings, for a diquark mass of 100 GeV. Understandably, the 2σ bounds are weaker than the 1σ ones. Similarly, the color-sextet couplings are more severely constrained than the color-triplet ones. As discussed above, for a few of the products there are two noncontiguous bands allowed. For the combination $h_{33}^{(4)}h_{32}^{(4)}$, though, the second window (both at the 1σ and 2σ levels) lies close to the perturbative limit and, hence, is phenomenologically uninteresting.

As discussed earlier, $\tilde{h}_{ij}^{(4)}$ is analogous to the trilinear R-parity violating coupling λ''_{ijk}. Thus the constraints on $\tilde{h}_{33}^{(4)}\tilde{h}_{32}^{(4)}$ are equivalent to those on the product $\lambda''_{3k2}\lambda''_{3k3}$. For each of these couplings, the best *individual* bound comes from the precision measurements at the Z pole [24,29], and amounts to $\lambda''_{3k2},\lambda''_{3k3}<0.50$ at the 1σ level for squark masses of 100 GeV. We thus do not do very well as far as this particular combination is concerned. This can be attributed to both the chirality and the color structure of the operator, each of which is ''unfavorable'' as far the $b\to s\gamma$ decay is concerned. For most of the other combinations though, we do *significantly better* than the product of individual bounds [24].

In our effort to compare with the results available in the literature, we have, until now, held the diquark mass to be 100 GeV and varied the strength of its coupling. In reality, though, a diquark is more likely to be somewhat heavier. For the sake of completeness, we next investigate the dependence on the diquark mass (Fig. 4), while holding the product fixed. As is expected, the extra contribution falls off with m_Φ. The falloff is somewhat slower than m_Φ^{-2} [see the expressions for $F_i(y)$ in Eq. (16)] and the effects persist till $m_\Phi \sim 3$ TeV. The different rates of falloff are governed by the dominant $F_i(y)$ in each case. The case for the combination $\tilde{h}_{33}^{(3)}h_{32}^{(3)}$ looks somewhat nontrivial. However, the shape is just a consequence of accidental cancellations between various terms of Eq. (19). As the extent of these cancellations depend crucially on the value of the diquark couplings, not much should be read into the shape in general or the minimum in particular. The two dependences (m_Φ and cou-

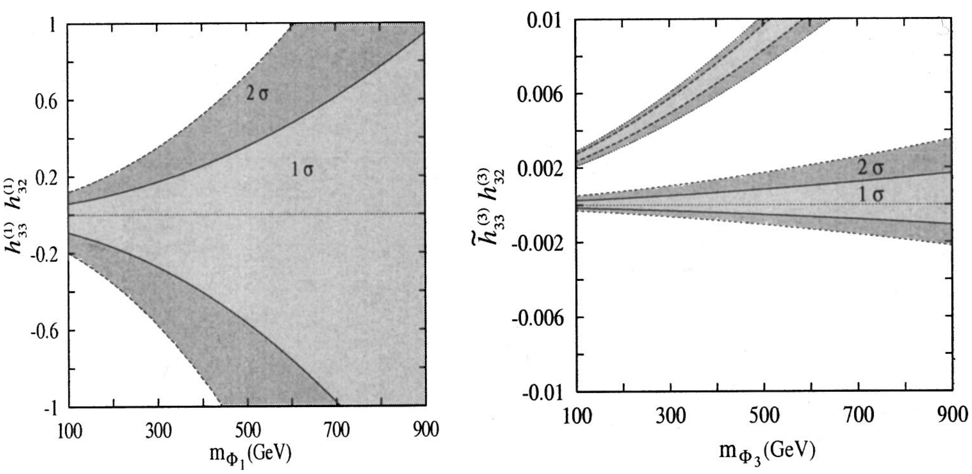

FIG. 5. The region of the parameter space allowed by the data when all other couplings are set to zero. The lightly shaded area agrees with the data at 1σ level, whereas the encompassing darker region agrees at 2σ.

pling strength) that we have studied can be combined to rule out parts of the parameter space. In Fig. 5, we exhibit this for two particular combinations. In each figure, the shaded regions of the parameter space are in agreement with the experimental results at the designated level. For $h_{33}^{(1)} h_{32}^{(1)}$, the second allowed region is beyond the perturbative limit.

In summary, we have studied the effects of the scalar diquark and/or R-parity violating coupling to the branching ratio $B \to X_s \gamma$. Amongst the possible new contributions, the scalar diquark mediated diagram yield promising effects. The precise measurement of this branching ratio at the upcoming B factories in near future and the reduction of theoretical uncertainty will only improve our limits on the product of different scalar diquark and/or R-parity violating couplings.

D. Choudhury acknowledges the Department of Science and Technology, India, for financial support.

[1] T. Inami and C. S. Lim, Prog. Theor. Phys. **65**, 297 (1981); **65**, 1772(E) (1981).
[2] B. Grinstein and M. B. Wise, Phys. Lett. B **201**, 274 (1988).
[3] H. Dreiner, Mod. Phys. Lett. A **3**, 867 (1988).
[4] S. Bertolini, F. Borzumati, A. Masiero, and G. Ridolfi, Nucl. Phys. **B353**, 591 (1991).
[5] A. Peterson, Phys. Lett. B **282**, 207 (1992).
[6] G. Bhattacharyya, G. C. Branco, and D. Choudhury, Phys. Lett. B **336**, 487 (1994).
[7] T. G. Rizzo, Phys. Rev. D **50**, 3303 (1994).
[8] A. Kundu, T. De, and B. Dutta-Roy, Phys. Rev. D **49**, 4801 (1994).
[9] G. Bhattacharyya and A. Raychaudhuri, Phys. Lett. B **357**, 119 (1995).
[10] E. Gabrielli and U. Sarid, Phys. Rev. Lett. **79**, 4752 (1997).
[11] E. Gabrielli and U. Sarid, Phys. Rev. D **58**, 115003 (1998).
[12] T. Besmer and A. Steffen, Phys. Rev. D **63**, 055007 (2001).
[13] M. Aoki, E. Asakawa, M. Nagashima, N. Oshimo, and A. Sugamoto, Phys. Lett. B **487**, 321 (2000).
[14] E. Gabrielli, S. Khalil, and E. Torrente-Lujan, Nucl. Phys. **B594**, 3 (2001).
[15] CLEO Collaboration, S. Ahmed *et al.*, CLEO CONF 99-10, hep-ex/9908022.
[16] ALEPH Collaboration, R. Barate *et al.*, Phys. Lett. B **429**, 169 (1998).
[17] A. L. Kagan and M. Neubert, Eur. Phys. J. C **7**, 5 (1999).
[18] F. Zwirner, Int. J. Mod. Phys. A **3**, 49 (1988); J. L. Hewett and T. G. Rizzo, Phys. Rep. **183**, 193 (1989), and references therein.
[19] H. P. Nilles, Phys. Rep. **110**, 1 (1989); H. E. Haber and G. L. Kane, *ibid.* **117**, 75 (1985); L. J. Hall and M. Suzuki, Nucl. Phys. **B231**, 419 (1984); S. Dawson, *ibid.* **B261**, 297 (1985); S. Dimopoulos and L. J. Hall, Phys. Lett. B **207**, 210 (1987).
[20] S. Weinberg, Phys. Rev. D **26**, 287 (1982); N. Sakai and T. Yanagida, Nucl. Phys. **B197**, 533 (1982).
[21] P. Fayet, Phys. Lett. **69B**, 489 (1977); G. Farrar and P. Fayet, *ibid.* **76B**, 575 (1978).
[22] K. Tamvakis, Phys. Lett. B **382**, 251 (1996).
[23] CDF Collaboration, F. Abe *et al.*, Phys. Rev. D **55**, 5263 (1997).
[24] G. Bhattacharyya, D. Choudhury, and K. Sridhar, Phys. Lett. B **355**, 193 (1995).
[25] B. Brahmachari and P. Roy, Phys. Rev. D **50**, R39 (1995); **51**, 3974(E) (1995).
[26] J. L. Goity and M. Sher, Phys. Lett. B **346**, 69 (1995).
[27] C. E. Carlson, P. Roy, and M. Sher, Phys. Lett. B **357**, 99 (1995).
[28] R. Barbieri and A. Masiero, Nucl. Phys. **B267**, 679 (1986).
[29] G. Bhattacharyya, talk given at Workshop on Physics Beyond the Standard Model: Beyond the Desert: Accelerator and Non-accelerator Approaches, Tegernsee, Germany, 1997, hep-ph/9709395.
[30] B. Grinstein, R. Springer, and M. B. Wise, Nucl. Phys. **B339**, 269 (1990).
[31] R. Grigjanis *et al.*, Phys. Rep. **228**, 93 (1993).
[32] A. Buras, Lectures given at Les Houches Summer School in Theoretical Physics, Session 68: Probing the Standard Model of Particle Interactions, Les Houches, France, 1997, edited by R. Gupta, A. Morel, E. de. Rafael, and F. David (North-Holland, Amsterdam, 1999).
[33] K. Chetyrkin, M. Misiak, and M. Münz, Phys. Lett. B **400**, 206 (1997); **425**, 414(E) (1998).